Published in final edited form as:
*Nat Cell Biol*. 2009 February ; 11(2): 219–225. doi:10.1038/ncb1830.

# Cytoplasmic penetration and persistent infection of mammalian cells by polyglutamine aggregates

**Pei-Hsien Ren**[1], **Jane E. Lauckner**[1], **Ioulia Kachirskaia**[1], **John E. Heuser**[3], **Ronald Melki**[2], and **Ron R. Kopito**[1,*]

[1]Department of Biology Stanford University Stanford, CA 94305-5020 USA

[2]Laboratoire d'Enzymologie et Biochimie Structurales Centre National de la Recherche Scientifique 91198 Gif-sur-Yvette France

[3]Department of Cell Biology and Physiology Washington University School of Medicine 660 South Euclid Avenue, St. Louis, Missouri 63110 USA

## Abstract

Sequence-specific nucleated protein aggregation is closely linked to the pathogenesis of most neurodegenerative diseases and constitutes the molecular basis of prion formation[1]. Here we report that fibrillar polyglutamine peptide aggregates can be internalized by mammalian cells in culture where they gain access to the cytosolic compartment and become co-sequestered in aggresomes together with components of the ubiquitin-proteasome system and cytoplasmic chaperones. Remarkably, these internalized fibrillar aggregates are able to selectively recruit soluble cytoplasmic proteins with which they share homologous, but not heterologous amyloidogenic sequences and to confer a heritable phenotype upon cells expressing the homologous amyloidogenic protein from a chromosomal locus.

Genetic expansion of CAG triplets in protein-coding regions of otherwise unrelated genes is the underlying cause of a family of dominantly inherited neurodegenerative diseases including Huntington disease (HD) and spinocerebellar ataxias[2]. The tracts of polyglutamine (polyQ) homopolymers ($Q \geq 40$) encoded by these expanded CAG triplets cause the normally soluble protein products of these genes, or fragments thereof, to form cytotoxic protein aggregates[2]. CAG expansion diseases therefore, belong to a much larger family of protein "conformational diseases," including systemic and organ-specific amyloidosis, Alzheimer's disease and prion encephalopathy. Pathogenesis in these diseases is tightly linked to the formation of high molecular weight, fibrillar, β-sheet rich, insoluble protein aggregates, termed "amyloid," that accumulate in characteristic sites either inside or outside of the cell[1, 3].

In amyloidosis, insoluble protein fibrils derived from normally soluble secreted proteins are deposited in the *extracellular* milieu causing damage to surrounding viscera, blood vessel walls and connective tissue[4]. Whether organ damage is a consequence of tissue disruption or obstruction due to the sheer mass of deposited protein, as in the case of systemic amyloidosis[4], or to an intrinsic cytotoxicity of amyloids or their oligomeric precursors, as in the case of neuropathic amyloidosis[5], remains a critical but unresolved question. In contrast to amyloidosis, most neurodegenerative diseases are caused by alterations in the conformation and oligomeric state of normally well-behaved *intracellular* proteins that, in diseased states, accumulate within cytoplasmic or nuclear inclusion bodies[6]. Emerging evidence suggests that oligomeric precursors to these large assemblies are cytotoxic and directly impair crucial

*corresponding author. Tel 650 723-7581 email: kopito@stanford.edu.

cellular functions which cause the neuronal dysfunction and ultimately death associated with these disorders[7].

Many extracellular amyloids and amyloid precursors, including those associated with systemic amyloidosis, neurodegenerative disease, and even those not associated with disease[7], can be taken-up by a wide variety of cell types including macrophages, neurons, fibroblasts, and epithelial cells[7-10]. This uptake is reported to occur via phagocytic or endocytic processes that result in delivery to lysosomes which may suppress their toxicity by degrading them[9, 10]. However, all of these mechanisms would deliver aggregates to an endomembrane compartment, and not to the cytosol. Surprisingly, a recent study reported that healthy fetal tissue grafted into the brains of Parkinson's disease patients, acquired cytoplasmic alpha-synuclein- rich Lewy bodies, suggesting a potential “prion-like” transmission of nucleating species from the recipient's diseased brain to the healthy grafted tissue[11].

The ability of amyloid to cross a membrane barrier and access the nucleocytoplasmic compartment, a necessary step to effect conversion of a cytoplasmic protein like α-synuclein by extracellular aggregates, has never been directly demonstrated. The starting point of the present work was the demonstration by Yang et al that fibrillar, insoluble amyloid formed from synthetic polyglutamine peptides or an amyloidogenic bacterial protein, Csp-B1, are readily taken up by mammalian cells in culture[8]. Those studies did not determine whether the “intracellular” amyloids were present within lysosomal or other endomembrane compartments- the demonstrated route for entry of other amyloids into mammalian cells- or the cytosol, which would necessitate the unlikely possibility that these large protein assemblies had crossed a biological membrane. Although they did not directly test this possibility, Yang et al[8] reported that exogenously administered amyloids to which a nuclear localization sequence (NLS) had been appended appeared to gain access to the nucleus, raising the possibility that at least some aggregate-associated NLS had become accessible to importins in the cytosol. We therefore sought to directly test whether large polyQ amyloid assemblies can move from outside the cell into the cytosol.

PolyQ peptides ($K_2Q_{44}K_2$), labeled with fluorescein, rhodamine or biotin were converted to fibrillar aggregates[12] that appeared by transmission electron microscopy to be composed of bundles of individual fibrils measuring 3-5 nm in width (Fig 1a,b) These polyQ amyloids have been extensively characterized and exhibit characteristic β-sheet circular dichroism spectra, bind thioflavin T and react with monoclonal antibodies to amyloid[13]. Fluorescent $K_2Q_{44}K_2$ aggregates were efficiently internalized by COS7 cells (Fig 1c) and by other cell lines including HEK293 and neuro2A (Figs 2-4) as well as CHO and HeLa S3 (not shown). Following overnight incubation with cells, $K_2Q_{44}K_2$ aggregates were enriched in a juxtanuclear, pericentriolar region that was labeled with antibodies to γ-tubulin (Fig 1d). Although this cellular region is enriched in late endosomes, lysosomes (Fig 1e) and autophagosomes (staining for LC3; not shown), we failed to detect any significant colocalization of aggregate foci with markers for these organelles. By contrast, strong colocalization was observed between internalized $K_2Q_{44}K_2$ aggregates and cytosolic `quality control' components including ubiquitin, proteasome subunits, and Hsp70 (Fig 1e), suggesting that internalized fibrillar polyQ aggregates did not accumulate within an endosomal compartment.

To investigate the possibility that the aggregates had gained access to the cytoplasmic compartment, we used deep-etch transmission electron microscopy of “unroofed”[14] cells that had been briefly exposed to polyQ aggregates (Fig 2a). These images reveal the presence of large fibrillar aggregates, which appear indistinguishable from those used to inoculate the cells, attached to the inner surface of the plasma membrane, resting on a “bed” of cortical actin. There was no evidence in these images that aggregates associated with, or were surrounded by, any endomembranous structures or clathrin.

To further assess whether externally applied polyQ amyloids are in direct contact with cytosolic proteins, we determined whether externally applied $K_2Q_{44}K_2$ aggregates are capable of nucleating the polymerization of a cytoplasmic polyQ rich protein "reporter", exploiting the well known ability of fibrillar polyQ amyloids to nucleate the polymerization of normally soluble proteins containing polyQ tracts below the threshold ($Q \leq \sim 37$) for spontaneous aggregation. Control experiments confirmed that $K_2Q_{44}K_2$ aggregates are capable of nucleating aggregation of bacterially-expressed glutathione S-transferase (GST) linked to the N-terminal exon of huntingtin (Htt) with either a non-pathogenic (18Q) or a pathogenic (51Q) repeat (Supplementary Information, Fig. S1, online). We therefore assessed the aggregation state of cyan fluorescent protein (CFP)-tagged Htt exon 1 (CFP-$HttQ_{25}$) in HEK293 cells following infection with extracellular aggregates (Fig. 2b). CFP fluorescence in untreated cells exhibited a diffuse nucleocytoplasmic distribution, as expected of a soluble $HttQ_{25}$ fragment (Fig. 2b). Strikingly, CFP fluorescence following infection with $K_2Q_{44}K_2$ aggregates redistributed into distinct foci (Fig. 2b) that colocalized extensively with the internalized $K_2Q_{44}K_2$ puncta. Quantification of the extent of colocalization indicated that nearly 90% of the $K_2Q_{44}K_2$ puncta were coincident with CFP puncta, suggesting that the intracellular and extracellular proteins had indeed coalesced into common intracellular foci. Conversion of the cytoplasmic reporter to a punctate distribution is first detectable within 1hr following exposure to aggregates (data not shown); this phenotype is present in more than 90% of reporter cells by 24 hr (Fig. 2d). To determine if the ability to convert diffuse cytoplasmic $Q_{25}$ to a punctate distribution is a property unique to aggregates generated from synthetic $Q_{44}$ peptides or a more general property of polyQ amyloids, aggregates were generated *in vitro* from purified, bacterially expressed Htt exon 1 containing either 18 or 51 glutamines (Fig. 2e). These assemblies were used to infect HEK293 cells stably expressing a $Q_{25}$ reporter fused to cherry fluorescent protein (chFP-$HttQ_{25}$). Reporter cells exposed to non-fibrillar $HttQ_{18}$ aggregates (Fig. 2e, inset) maintained a diffuse pattern of fluorescence (Fig. 2e, f). By contrast, reporter cells exposed to highly fibrillar $HttQ_{51}$ aggregates (Fig. 2e, inset) exhibited extensive conversion to a punctate distribution (Fig. 2e, f). These data indicate that cell penetration and cytosolic nucleation is a property common to fibrillar polyQ amyloids and not simply an artifact of amyloids produced from synthetic peptides.

We used a filter retardation assay to confirm that the observed coalescence of CFP fluorescence into puncta reflects a change in the aggregation state of CFP-$HttQ_{25}$ (Fig. 2g). In control samples not exposed to added aggregates, filter-bound CFP-$HttQ_{25}$ was undetectable, while GFP-$HttQ_{71}$ could be weakly detected, reflecting spontaneous aggregation owing to its longer polyQ tract. However, in cells exposed to $K_2Q_{44}K_2$ fibrils, GFP-$HttQ_{25}$ and, to a greater extent, GFP-$HttQ_{71}$, were readily trapped by the filter, confirming that the observed changes in reporter distribution reflect a change in the overall aggregation state of the intracellular protein. Addition of an equivalent amount of $Q_{44}$ fibrils to cells during lysis was largely ineffective at inducing aggregation of the cellular reporters, indicating that the observed conversion of the endogenous intracellular reporter is not an artifact of sample preparation. $K_2Q_{44}K_2$ aggregates were also observed to induce focal redistribution (Supplementary Information, Fig. S2a, online) and aggregation (Supplementary Information, Fig. S2b, online) of cytoplasmic GFP-$HttQ_{60}$ expressed in differentiated, postmitotic neuro2A neuroblastoma cells[15]. Together, these observations strongly suggest that fibrillar polyQ aggregates can enter the cytosolic compartment of mammalian cells where they nucleate the aggregation of otherwise soluble proteins containing polyQ tracts.

Sequence-specificity of amyloid nucleation is a fundamental property that underlies the species barrier and strain selectivity properties of prions in both mammals[16] and yeast[17]. To test whether the proposed intracellular nucleation of cytoplasmic Htt is selective for proteins with polyQ tracts, we generated fibrillar aggregates from two well-characterized amyloids, the prion domain of the yeast Sup35 prion protein (Sup35-NM) and the Alzheimer's disease amyloid

peptide Aβ(1-40) (Supplementary Information,Fig. S3, online). These aggregates were efficiently internalized by cells and accumulated in a juxtanuclear distribution (Fig. 3a), which, like the $K_2Q_{44}K_2$ aggregates, colocalized with ubiquitin and proteasome epitopes (not shown). To assess the selectivity of nucleation of CFP-Htt$Q_{25}$ aggregation we repeated the infection experiment using either `homologous' ($K_2Q_{44}K_2$) or `heterologous' (Sup35-NM or Aβ(1-40)) aggregates. When cells expressing CFP-Htt$Q_{25}$ were incubated with either Sup35-NM or Aβ (1-40) aggregates, CFP-Htt$Q_{25}$ fluorescence remained diffuse and homogeneous, indistinguishable from untreated cells, while cells infected with $K_2Q_{44}K_2$ aggregates exhibited a punctate redistribution of CFP-Htt$Q_{25}$ (Fig. 3b). The heterologous aggregates were unable to induce aggregation of GFP-Htt$Q_{25}$ or GFP-Htt$Q_{71}$ in the filter retardation assay (Fig. 3c), strongly supporting the conclusion that the ability of exogenously added aggregates to nucleate cytoplasmic polyQ aggregation is sequence-specific.

To determine whether selective nucleation of homologous cytoplasmic proteins by internalized fibrillar aggregates is an exclusive characteristic of polyQ-containing proteins we tested the ability of Sup35-NM aggregates to induce the specific aggregation of a cytoplasmically expressed GFP-Sup35-NM reporter (Fig. 3d). In the absence of added aggregates, the vast majority of GFP-Sup35-NM remained soluble. By contrast, the protein shifted mostly to the insoluble pellet fraction in cells treated with Sup35-NM, but not $K_2Q_{44}K_2$ or Aβ(1-40) aggregates. Therefore, the ability of extracellular fibrillar amyloids to nucleate the aggregation of cytoplasmic proteins in a specific, template-dependent manner in mammalian cells is not an exclusive property of polyQ aggregates and of proteins containing homopolymeric polyQ tracts.

To determine whether the novel phenotype of CFP-Htt$Q_{25}$ expressing cells infected with $K_2Q_{44}K_2$ aggregates can be inherited during cell division, we transiently exposed a population of HEK293 cells stably expressing CFP-Htt$Q_{25}$ to extracellular tetramethylrhodamine (TMR)-labeled $K_2Q_{44}K_2$ aggregates and quantified the fraction of cells with the novel, punctate CFP fluorescence phenotype in subsequent generations (Fig. 4a). The fraction of $K_2Q_{44}K_2$ aggregate-infected cells exhibiting this phenotype declined exponentially over the first 15-20 generations after infection, in parallel with the measured loss of fluorescent $K_2Q_{44}K_2$ aggregates, suggesting that the initial inoculum was diluted during cell division. The frequency of cells beyond generation 27 with CFP-Htt$Q_{25}$ puncta was consistently and significantly ($P = 0.004$) higher at each generation following infection with $K_2Q_{44}K_2$ aggregates than after control treatments with dextran or Aβ amyloid (Fig. 4b). Moreover, cells initially exposed to a ten-fold lower $K_2Q_{44}K_2$ aggregate inoculum (0.1μM) also sustained a persistent punctate phenotype that was quantitatively indistinguishable from that induced by the higher concentration of $K_2Q_{44}K_2$ aggregates. Thus, persistent aggregation of a strictly nucleocytoplasmic polyQ reporter is a novel and heritable phenotype of cells transiently exposed to extracellularly administered homotypic, but not heterotypic, protein aggregates.

We propose that the persistence of the CFP-Htt$Q_{25}$ aggregate phenotype at low but significant levels through multiple generations in $K_2Q_{44}K_2$ aggregate-treated mammalian cells reflects the existence of an efficient mechanism to suppress the distribution of cytoplasmic aggregates during cell division or the dissemination of aggregates to neighboring cells following cell lysis. Internally formed polyQ aggregates are efficiently sequestered into pericentriolar aggresomes that are only rarely (~1% of the time) segregated equally among mitotic progeny during cell division[18]. Perhaps aggresome formation is a mechanism that has evolved to minimize prion propagation among dividing cells.

The observation of a persistent aggregation phenotype in dividing cells implies that aggregates formed within mammalian cells are themselves capable of nucleating aggregation when distributed through cytoplasmic transfer during cytokinesis. However, in order to be potentially

relevant to the pathogenesis of neurological diseases such as HD, in which the target cells are post-mitotic neurons, aggregates formed within a mammalian cell must be able to translocate to neighboring uninfected cells. When HEK reporter cells stably expressing a cherry fluorescent protein-tagged Htt fragment (chFP-$HttQ_{25}$) were co-cultured together with HEK cells stably expressing GFP-$HttQ_{71}$, the vast majority of the $HttQ_{25}$ reporter retained a diffuse cytoplasmic pattern of fluorescence, despite the presence of highly aggregated $HttQ_{71}$ foci in neighboring cells (Fig. 4c). Quantification of the fraction of $HttQ_{25}$ cells with chFP puncta revealed that cells co-cultured with GFP-$HttQ_{71}$ exhibited a slightly higher number of chFP-$Q_{25}$ puncta compared with reporter cells grown alone or co-cultured with GFP-$HttQ_{25}$ (Fig. 4d), possibly due to inefficient transfer of aggregates through cell-cell contact or to uptake of aggregates released by GFP-$HttQ_{71}$ cells. By contrast, we found that selective lysis of GFP-$HttQ_{71}$ cells with puromycin (the reporter cells are genetically resistant to the drug) gave rise to a striking increase in the number of cells with chFP-$HttQ_{25}$ puncta (Figs 4c,d). No such increase was observed when co-cultured HEK cells expressing GFP-$HttQ_{25}$ were killed with puromycin (Fig. 4d). The precise colocalization of chFP cytoplasmic puncta with GFP fluorescence strongly argues that $HttQ_{71}$ aggregates from the lysed cells were internalized by the reporter cells and that the internalized aggregates are capable of nucleating homotypic aggregation of the GFP-$HttQ_{25}$ reporter.

The data reported here establish that cell membranes are far more permeable to large fibrillar aggregates than hitherto suspected. Although other investigators have reported that fibrillar aggregates can be internalized by mammalian cells and sequestered within the endosomal/lysosomal compartment[7-10], our study directly demonstrates penetration of the cytoplasmic compartment by fibrillar aggregates. Perhaps large, rigid polyQ amyloid fibrils are able to physically breach biological membranes, as has been reported for spherical prefibrillar oligomers of amyloidogenic proteins[19, 20]. It is unlikely in our experiments that fibrillization of polyQ aggregates occurs directly at the cell surface, as has been proposed for insulin associated polypeptide, IAPP[21], as our preparations are largely devoid of monomer. Further research is clearly necessary to understand the mechanism by which these large proteinaceous assemblies are able to gain access to the cytoplasm.

These findings thus have broad implications for understanding the pathogenesis of the large number of human disorders —including Alzheimer's disease and systemic amyloidosis— that are associated with the deposition of cytotoxic amyloids in the extracellular space. The recent discovery that alpha-synuclein-positive Lewy bodies can be propagated from diseased tissue to healthy transplanted fetal mesencephalic dopaminergic neurons in human Parkinson's disease brains[11] strongly suggests that passage of aggregated pathogenic proteins between cells within an individual brain may contribute to the pathogenesis of Parkinson's disease. Our data suggest the possibility that this sort of mechanism may also contribute to polyglutamine diseases- and perhaps other neurodegenerative diseases as well.

## Methods

### Peptides

The $K_2Q_{44}K_2$ and Aβ (1-40) peptides used in these experiments were prepared by Fmoc chemistry at the Keck Biotechnology Resource Laboratory of Yale University. The polyQ peptides used in this study were flanked by pairs of lysine residues to improve solubility as described[12]. $K_2Q_{44}K_2$ was synthesized with FITC, TMR, or biotin conjugated via the ε-amino group of the N-terminal lysine. The α-amino group of Aβ (1-40) was conjugated to biotin.

## Antibodies

Monoclonal rab9 antibody was a kind gift from Dr. Suzanne Pfeffer (Stanford University). Polyclonal cathepsin D antibody was purchased from Oncogene (San Diego, CA). Monoclonal GFP antibody was purchased from Roche (Mannheim, Germany). Ubiquitin polyclonal antibodies were from Chemicon International (Temecula, CA). Polyclonal Hsp70 antibody was from Assay Designs. Monoclonal proteasome S7 antibody was obtained from Biomol. Monoclonal γ-tubulin was purchased from Sigma. Monoclonal antibody to LAMP1 was obtained from the Iowa Hybridoma Bank.

## Aggregate Preparation

PolyQ peptide aggregates were generated as previously described[12, 22]. Lyophilized Aβ (1-40) peptides were solubilized in 2% (v/v) trifluoroacetic acid in hexafluoroisopropanol overnight. Solvents were evaporated under a stream of nitrogen. Peptides were resuspended in 10 mM phosphate buffer, pH 7.4, and aged at 37°C for 3 days. Sup35-NM aggregates were a generous gift of Sean Collins and Jonathan Weissman (UCSF) and were prepared as previously described[23]. All aggregates were freshly sonicated on ice with a microtip sonicator using six pulses of 30 sec each at the highest power setting before use. GST-Htt$Q_{51}$ aggregates were prepared as previously described[24]. Aggregates were suspended in phosphate buffer saline (PBS) for incubation with cells. Mock treated cells were incubated with PBS only.

Recombinant His-tagged MBP-TEV-Htt$Q_{18}$ and $_{51}$ were purified using Talon metal affinity resin. The fusion proteins (3mg/ml) were incubated for 2h at room temperature with 0.05mg/ml MBP-TEV. The reaction mixture was incubated at 4°C with amylose resin for 3h. The flow-through was collected and its purity assessed using 12% SDS-PAGE. Amyloid assembly was achieved by incubating purified Htt$Q_{18}$ and $_{51}$ at 37°C under agitation (200rpm) for 48 hours.

## Thioflavin T Binding

Thioflavin T binding was measured as previously described[13]. Briefly, 10 μL of 2.5 mM thioflavin T was added to 290 μL of aggregated polyQ peptide in PBS and equilibrated for 10 min at room temperature. This solution was then transferred to a quartz cuvette and an emission spectrum from 460 nm to 560 nm was obtained in a fluorometer with an excitation wavelength of 450 nm. Excitation slit width was set at 2.6 nm and emission slit width was at 9 nm.

## Electron Microscopy

Transmission electron micrographs were acquired at the Cell Sciences Imaging Facility at Stanford University, using either a JEM 1010 or a Philips CM120 electron microscope at 80 kV excitation voltage. 5 μL of peptide or protein aggregates were placed on carbon/formvar coated Cu grids. The grids were then stained with 1% uranyl acetate in dd$H_2O$ for 1 min. For "deep-etch" electron microscopy[25], polyQ aggregates were spun down onto small glass coverslips at 1000×g in a swinging-bucket centrifuge, after which the coverslips were fixed in 2% glutaraldehyde freshly dissolved in 100 mM NaCl, 30 mM HEPES buffer pH 7.4, and 2 mM $CaCl_2$. The coverslips were then washed several times in distilled water, quick-frozen with a homemade liquid-helium cooled, copper cold block "slammer," freeze dried *in vacuo* at minus 80°C for 15 min, replicated with a ~2 nm film of platinum vacuum-evaporated from an electron beam gun mounted 15-20° above the horizontal, and supported or "backed" by vacuum-evaporating ~10 nm of pure carbon onto the Pt, using a standard carbon-arc supply mounted some 10° off the vertical. The resultant Pt replicas of polyQ aggregates were floated off the glass by angled immersion into full strength (47%) hydrofluoric acid, washed several times by floatation on distilled water, picked up on 75 mesh formvar-coated EM grids, and imaged at 50,000x while mounted in a eucentric side-entry goniometer stage of a JEOL 200CX electron microscope.

### Cell Culture

Human embryonic kidney (HEK)293, COS7, and Neuro-2A cells were cultured in Dulbecco's Modified Eagle Medium supplemented with 10% fetal bovine serum at 37°C in 5% $CO_2$. Plasmid transfection was performed using either the calcium phosphate method or Lipofectamine 2000. Cells were exposed to aggregated peptides or proteins ~40 hours post transfection. Cells were lysed in 0.5% NP-40, 100 mM NaCl, 50 mM Tris-HCl pH 8.8, 5 mM $MgCl_2$, 1 mM EDTA with protease inhibitor cocktail tablets (Roche). Clonal cell lines of GFP-$httQ_{25}$, GFP-$httQ_{71}$, CFP-$httQ_{25}$ and chFP-$httQ_{25}$ were selected and maintained at 400 μg/mL of G418. Neuro-2A cell lines with inducible GFP-$httQ_{60}$, was a generous gift from Dr. Nobuyuki Nukina (RIKEN, Japan)[15].

### Immunofluorescence Microscopy

COS7 cells were incubated for 60 min with 0.5 μM monomer equivalents of TMR-$K_2Q_{44}K_2$, alexa-546-Sup35-NM, or biotin-Aβ (1-40) aggregates at 4°C. Cells were washed and "chased" in complete growth medium at 37°C for 8 hours before fixation with 4% paraformaldehyde. Cells stained for γ-tubulin were fixed by methanol precipitation at -20°C for 10 minutes and did not undergo Triton X-100 permeabilization. Paraformaldehyde-fixed cells on poly-L-lysine-coated coverslips were permeabilized with 0.1% Triton X-100 in PBS for 3 minutes, washed, and blocked with 2% BSA in PBS for 30 minutes. Cells on coverslips were incubated with antibodies to ubiquitin, cathepsin D, hsp70, proteasome S7, γ-tubulin, or LAMP1 in 2% BSA for 1 hour. Antibodies to mouse or rabbit IgG conjugated to Alexa 488 or 594 were used as secondary antibodies. Biotin-Aβ (1-40) was visualized using Alexa-594 streptavidin. Nuclei were stained with 10 μg/ml bisbenzimide. Plasma membrane was stained using Oregon Green wheat germ agglutinin (Invitrogen) diluted 1:100 dilution in PBS on coverslips for 1 min before fixation.

### Fluorescence Microscopy

Cells were imaged by epifluorescence on a Zeiss Axiovert 200M microscope with a 100X oil lens (NA1.4; Zeiss). Digital (12-bit) images were acquired with a cooled CCD (Roper Scientific, Trenton, NJ) and processed using Metamorph software (Universal Imaging, Media, PA). The excitation filters used for epifluorescence microscopy were 365WB50 (bisbenzimide), 440AF21 (CFP), 500AF25 (GFP, Alexa488), and 560AF55 (Alexa546). Emission filters were 450 DF65 (bisbenzimide), 480 AF30 (CFP), 545AF35 (GFP, alexa488), 645DF55 (Alexa546). The dichroics were: 400 DCLP (bisbenzimide), 455DRLP (CFP), 525 DRLP (GFP, Alexa488), and 595 DRLP (Alexa546).

### Filter Retardation Assay

Cells were washed in PBS, harvested in PBS supplemented with 10 mM EDTA, and pellets were frozen in liquid nitrogen prior to analysis. Filter retardation assays were performed as previously described[26, 27]. Briefly, the pellets were solubilized in 0.5% NP-40 lysis buffer with protease inhibitor cocktail tablets (Roche). After centrifugation for 10 min at 20,000×g at 4° C, pellets were treated with DNase I for 1 hr at 37°C. Incubations were terminated by adjusting the mixtures to 20 mM EDTA, 2% SDS, and 50 mM DTT, following by heating at 100°C for 5 min. The resulting solutions were filtered through cellulose acetate membrane previously equilibrated with 0.1% SDS and washed with 0.1% SDS twice. Immunoblots were performed using antibody to GFP (Roche) or S-protein HRP (Novagen) as indicated.

### Sup35-NM Infection

Protein and peptide aggregates (1 μM monomer equivalent) were added to HEK293 cells ~40 hrs after transient transfection with GFP-Sup35-NM and incubated at 37°C for 24 hr. Cells were washed with PBS and collected in a pellet, which was then frozen in liquid nitrogen. For

a post-lysis control, freshly sonicated Sup35-NM aggregates were added to cells before freezing. Cells were stored at -80°C, resuspended in lysis buffer on ice and sonicated on ice using a microtip for 10 seconds at the highest power setting. Cell lysates were centrifuged at 17,000 ×g at 4°C for 20 min. Supernatants were collected and the pellets were washed with lysis buffer twice. Pellets were resuspended in 2X SDS sample buffer, vortexed, and heated at 100°C for 5 min. 20-50 μg of supernatant and an equivalent fraction of pellet were loaded per lane onto a 10-12% SDS-PAGE gel. Proteins were transferred onto PVDF membrane and immunoblotted with antibody to GFP. ECL-Plus was used to develop the blot and Typhoon was used to quantify band intensities.

### Propagation Experiment

In order to assess the hereditability of the $K_2Q_{44}K_2$-induced punate phenotype, 1 μM TMR-$K_2Q_{44}K_2$ aggregates were added to HEK293 cells stably expressing CFP-Htt$Q_{25}$ at generation "0." 1 μM TMR-$K_2Q_{44}K_2$ aggregates were added to HEK293 cells stably expressing CFP-Htt$Q_{25}$ at generation "0." Cells were split into new chambers with new coverslips roughly every 3 days. Cells on coverslips were washed with PBS and fixed with 4% paraformaldehyde. Cells with CFP puncta were scored from ≥ 500 cells in randomly selected fields by epifluorescence microscopy. The amount of cell-associated $K_2Q_{44}K_2$ was determined by direct measurement of the fluorescence of a population of cells exposed to 1 μM FITC-$K_2Q_{44}K_2$ aggregates compared against the fluorescence of fluorescein standards. The number of generations required to dilute this inocculum to less than 1 unit per cell, if we assume, conservatively, that a unit of inheritance is a single $K_2Q_{44}K_2$ monomer and that it partitions evenly to daughter cells, would be 22 generations. Since it is likely that a fibrillar amyloid is composed of many thousands of monomers, the actual number of generations is certain to be considerably smaller (12 generations if we assume uniform aggregates of 1000 monomers each). The phenotype frequencies shown in Fig. 4b were fitted to a generalized least squares model with a single predictor being the group indicator, and with an AR-1 correlation structure with coefficient 0.58 (estimated by an autoregressive model), giving a P-value for the data set for generations 22-87 of 0.004. Analysis of the data without accounting for the potential autocorrelation structure utilized a 2-group t-test yielding a P-value = 1.5e-6. P-values for data from two additional experiments were 2.7e-6 and 9.2e-7.

### Co-culture experiment

HEK293 cells stably expressing chFP-Htt$Q_{25}$ and puromycin resistance were grown on poly-L-lysine coverslips in Dulbecco's Modified Eagle Medium supplemented with 10% fetal bovine serum and 400 μg/mL of G418 at 37°C in 5% $CO_2$ in the presence of different densities of HEK cells stably expressing either GFP-Htt$Q_{71}$ or GFP-Htt$Q_{25}$ for 24h. Puromycin (4μg/ml) was then added to a subset of these cells which were further incubated for 48h. Cells on coverslips were washed with PBS and fixed with 4% paraformaldehyde. Cells with chFP puncta were scored in randomly selected fields by epifluorescence microscopy.

## Supplementary Material

Refer to Web version on PubMed Central for supplementary material.

## Acknowledgements

WWe thank J. Perrino and J. Mulholland for help with EM and confocal microscopy, K. Kirkegaard for comments on the manuscript, and G. Chang and T. Hastie for statistical analysis. This research was supported in part by a grant from the NINDS and a Stanford Graduate Fellowship to P-HR. RM is supported by the CNRS and the ANR contract # ANR-06-BLAN-0266.

## References


1. Chiti F, Dobson CM. Protein misfolding, functional amyloid, and human disease. Annu Rev Biochem 2006;75:333–366. [PubMed: 16756495]
2. Taylor JP, Hardy J, Fischbeck KH. Toxic proteins in neurodegenerative disease. Science 2002;296:1991–1995. [PubMed: 12065827]
3. Carrell RW, Lomas DA. Conformational disease. Lancet 1997;350:134–138. [PubMed: 9228977]
4. Pepys MB. Amyloidosis. Annu Rev Med 2006;57:223–241. [PubMed: 16409147]
5. Sousa MM, Cardoso I, Fernandes R, Guimaraes A, Saraiva MJ. Deposition of transthyretin in early stages of familial amyloidotic polyneuropathy: evidence for toxicity of nonfibrillar aggregates. Am J Pathol 2001;159:1993–2000. [PubMed: 11733349]
6. Ross CA, Poirier MA. Protein aggregation and neurodegenerative disease. Nat Med 2004;10 (Suppl):S10–17. [PubMed: 15272267]
7. Bucciantini M, et al. Inherent toxicity of aggregates implies a common mechanism for protein misfolding diseases. Nature 2002;416:507–511. [PubMed: 11932737]
8. Yang W, Dunlap JR, Andrews RB, Wetzel R. Aggregated polyglutamine peptides delivered to nuclei are toxic to mammalian cells. Hum Mol Genet 2002;11:2905–2917. [PubMed: 12393802]
9. Morten IJ, Gosal WS, Radford SE, Hewitt EW. Investigation into the role of macrophages in the formation and degradation of beta2-microglobulin amyloid fibrils. J Biol Chem 2007;282:29691–29700. [PubMed: 17686767]
10. Lee HJ, et al. Assembly-dependent endocytosis and clearance of extracellular alpha-synuclein. Int J Biochem Cell Biol 2008;40:1835–1849. [PubMed: 18291704]
11. Li JY, et al. Lewy bodies in grafted neurons in subjects with Parkinson's disease suggest host-to-graft disease propagation. Nat Med 2008;14:501–503. [PubMed: 18391963]
12. Chen S, Wetzel R. Solubilization and disaggregation of polyglutamine peptides. Protein Sci 2001;10:887–891. [PubMed: 11274480]
13. Chen S, Berthelier V, Hamilton JB, O'Nuallain B, Wetzel R. Amyloid-like features of polyglutamine aggregates and their assembly kinetics. Biochemistry 2002;41:7391–7399. [PubMed: 12044172]
14. Heuser J. The production of 'cell cortices' for light and electron microscopy. Traffic 2000;1:545–552. [PubMed: 11208142]
15. Jana NR, Tanaka M, Wang G, Nukina N. Polyglutamine length-dependent interaction of Hsp40 and Hsp70 family chaperones with truncated N-terminal huntingtin: their role in suppression of aggregation and cellular toxicity. Hum Mol Genet 2000;9:2009–2018. [PubMed: 10942430]
16. Cohen FE. Protein misfolding and prion diseases. J Mol Biol 1999;293:313–320. [PubMed: 10550211]
17. Santoso A, Chien P, Osherovich LZ, Weissman JS. Molecular basis of a yeast prion species barrier. Cell 2000;100:277–288. [PubMed: 10660050]
18. Rujano MA, et al. Polarised asymmetric inheritance of accumulated protein damage in higher eukaryotes. PLoS Biol 2006;4:e417. [PubMed: 17147470]
19. Kayed R, et al. Permeabilization of lipid bilayers is a common conformation-dependent activity of soluble amyloid oligomers in protein misfolding diseases. J Biol Chem 2004;279:46363–46366. [PubMed: 15385542]
20. Porat Y, Kolusheva S, Jelinek R, Gazit E. The human islet amyloid polypeptide forms transient membrane-active prefibrillar assemblies. Biochemistry 2003;42:10971–10977. [PubMed: 12974632]
21. Khémtemourian L, Killian JA, Hoppener JW, Engel MF. Recent insights in islet amyloid polypeptide-induced membrane disruption and its role in beta-cell death in type 2 diabetes mellitus. Exp Diabetes Res 2008;2008:421287. [PubMed: 18483616]
22. Chen S, Berthelier V, Yang W, Wetzel R. Polyglutamine aggregation behavior in vitro supports a recruitment mechanism of cytotoxicity. J Mol Biol 2001;311:173–182. [PubMed: 11469866]
23. DePace AH, Santoso A, Hillner P, Weissman JS. A critical role for amino-terminal glutamine/asparagine repeats in the formation and propagation of a yeast prion. Cell 1998;93:1241–1252. [PubMed: 9657156]

24. Scherzinger E, et al. Self-assembly of polyglutamine-containing huntingtin fragments into amyloid-like fibrils: implications for Huntington's disease pathology. Proc Natl Acad Sci U S A 1999;96:4604–4609. [PubMed: 10200309]

25. Heuser J. Three-dimensional visualization of coated vesicle formation in fibroblasts. J Cell Biol 1980;84:560–583. [PubMed: 6987244]

26. Wanker EE, et al. Membrane filter assay for detection of amyloid-like polyglutamine- containing protein aggregates. Methods Enzymol 1999;309:375–386. [PubMed: 10507036]

27. Scherzinger E, Lurz R, Turmaine M, Mangiarini L, Hollenbach B, Hasenbank R, Bates G, Davies SW, Lehrach H, Wanker E. Huntingtin-Encoded Polyglutamine Expansions Form Amyloid-like Protein Aggregates in Vitro and in Vivo. Cell 1997;90:549–558. [PubMed: 9267034]

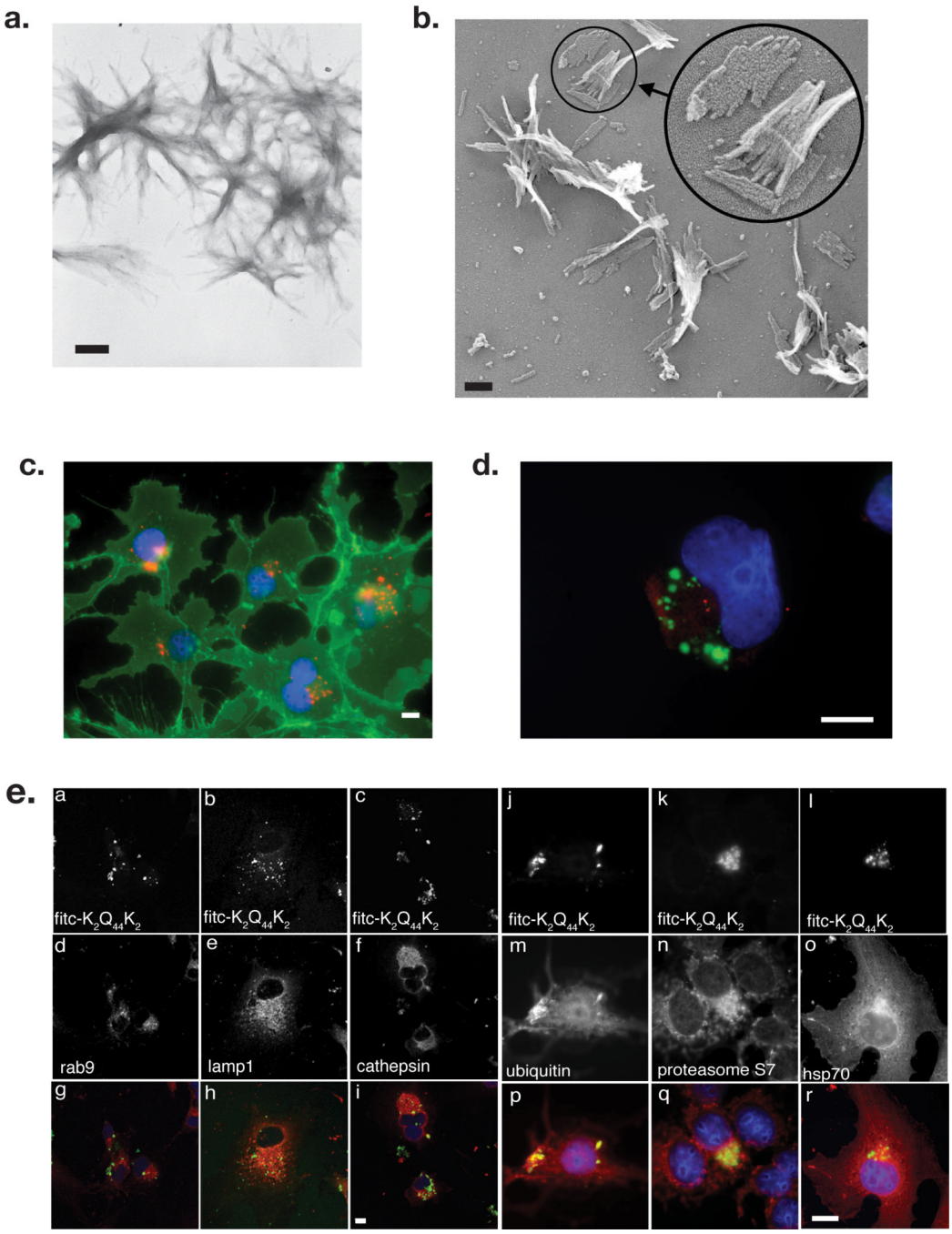


**Figure 1. Synthetic polyglutamine peptides form filamentous aggregates that are internalized by mammalian cells in culture**

A. Transmission electron micrograph of $K_2Q_{44}K_2$ aggregates stained with uranyl acetate. Bar = 200 nm.

B. "Deep-etch" transmission electron micrograph of $K_2Q_{44}K_2$ aggregates. Bar = 100 nm.

C. Juxtanuclear localization of $K_2Q_{44}K_2$ aggregates (red). Plasma membrane was labeled with wheat germ agglutinin (green) and nuclei with bisbenzimide (blue). Bar = 2 μm.

D. Pericentriolar distribution of $K_2Q_{44}K_2$ aggregates. COS7 cells were incubated with FITC-$K_2Q_{44}K_2$ aggregates (green). Fresh medium was replenished after 1 hour and cells chased

overnight. Following fixation cells were stained with antibody to γ-tubulin (red) and bisbenzimide (blue). Scale bars = 2 μm.

E. Comparison of internalized $K_2Q_{44}K_2$ aggregates with intracellular markers. Confocal micrographs of COS7 cells exposed to FITC-$K_2Q_{44}K_2$ for 10 hours. Cells were fixed and stained with antibodies against the indicated endolysosomal markers (d-f) or cytoplasmic quality control components (m-p). Cell nuclei were stained with bisbenzimide. Scale bar for panels a-i = 10 μm; for panels j-s = 2 μm.

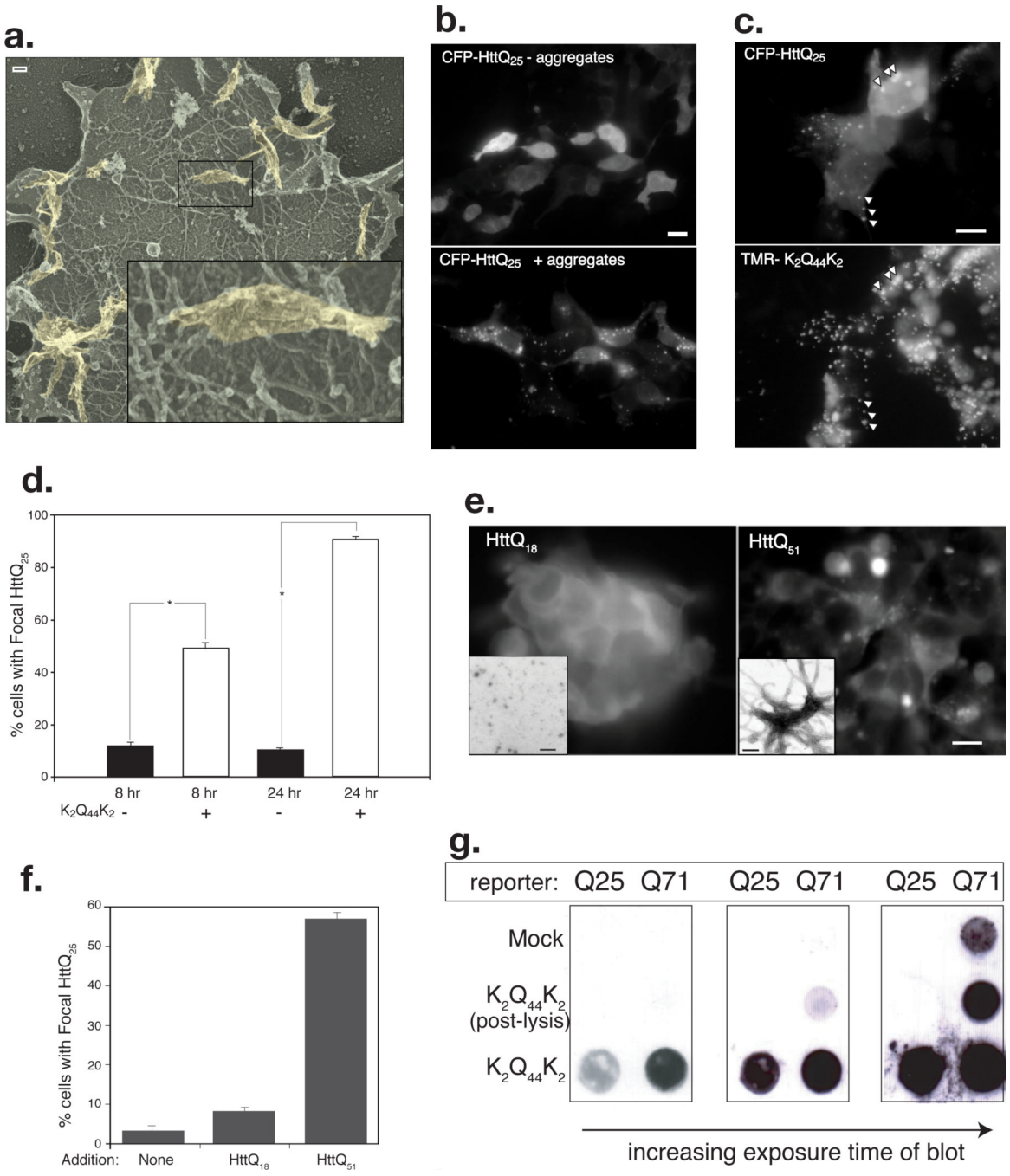


**Figure 2. Internalized polyglutamine peptide aggregates access the cytosolic compartment**

A. Internalized $K_2Q_{44}K_2$ aggregates are visible attached to the actin cortex of unroofed HEK293 cells visualized by deep-etch TEM. Inset higher magnification view of region indicated by box.

B. $K_2Q_{44}K_2$ aggregates induce focal redistribution of intracellular $HttQ_{25}$. Diffuse distribution of CFP-$HttQ_{25}$ fluorescence in cells incubated without aggregates (top) is converted to a punctate pattern following overnight exposure to aggregated TMR-$K_2Q_{44}K_2$ (bottom). Scale bar = 2 μm.

C. Colocalization of CFP-$HttQ_{25}$ puncta and TMR-$K_2Q_{44}K_2$. Scale bars = 2 μm.

D. Coalescence of CFP-Htt$Q_{25}$ fluorescence into puncta following infection with $K_2Q_{44}K_2$ aggregates. Cells ($n \geq 250$) exposed to TMR-$K_2Q_{44}K_2$ aggregates (white bars) or control (black bars) were scored for punctate CFP-Htt$Q_{25}$ appearance. Asterisk, $P$- $\leq 0.001$. Data representative of three independent experiments.

E. Fibrillar aggregates composed of bacterially expressed, purified Htt$Q_{51}$ are able to induce conversion of cytosolic chFP-$Q_{25}$ reporter. Scale bar = 2 μm. Insets, appearance of protein assemblies of Htt$Q_{18}$ (left) or Htt$Q_{51}$ (right) by negative stain EM. Scale bars = 20 nm.

F. Quantification of data from experiment in Fig. 2D. Number of cells counted in each experiment ≥300 cells.

G. $K_2Q_{44}K_2$ aggregates induce aggregation of intracellular Htt. HEK293 cells stably expressing GFP-Htt$Q_{25}$ or $Q_{71}$ were infected with $K_2Q_{44}K_2$ aggregates for 24 hours prior to filter retardation assay. Post-lysis control is explained in Methods. Data representative of 3 independent experiments.

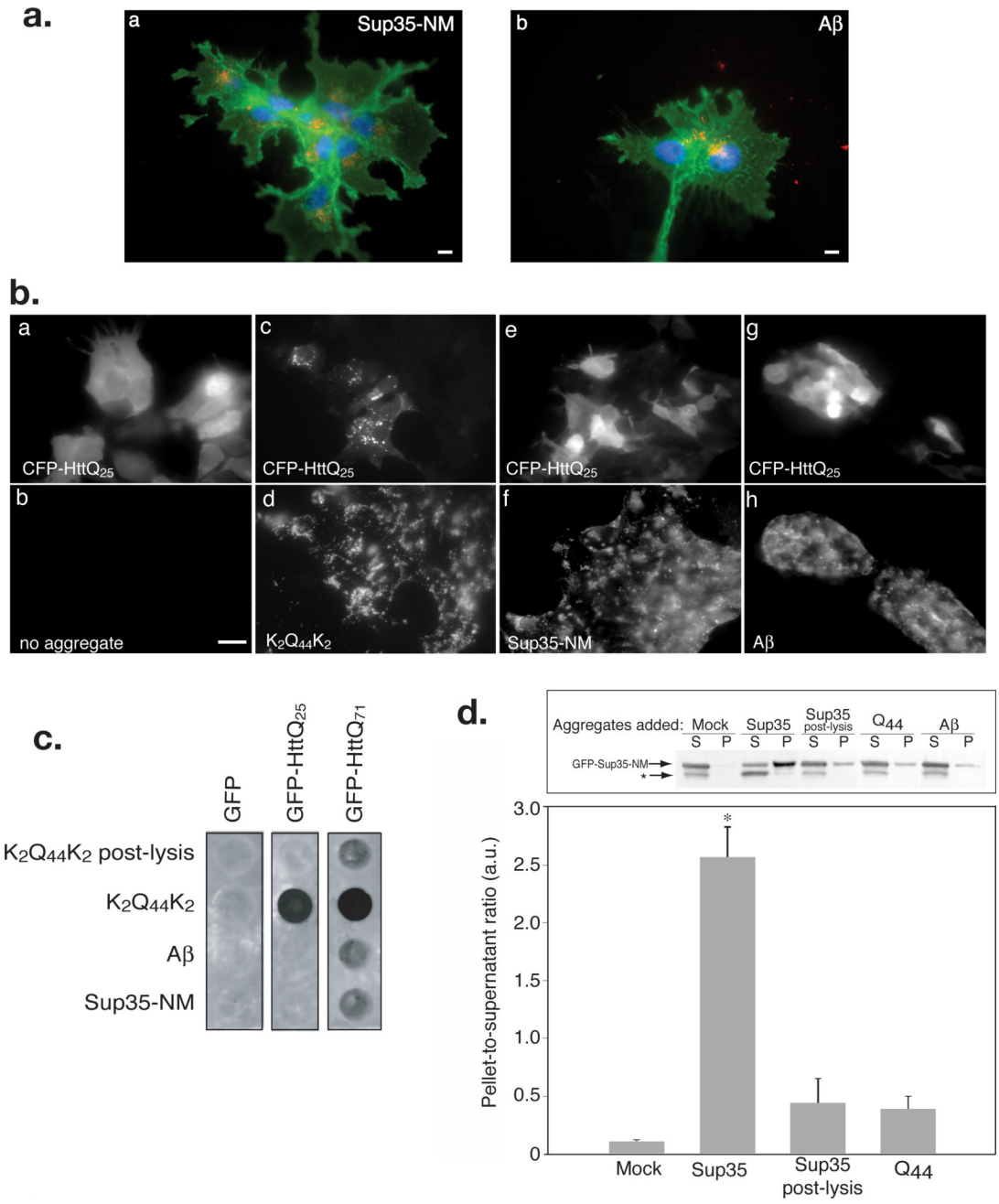


**Figure 3. Internalized fibrillar aggregates induce homotypic but not heterotypic aggregation of cytoplasmic reporters**

A. Sup35-NM and Aβ aggregates are internalized by mammalian cells. COS7 cells were infected with aggregated Sup35-NM (red; a) or Aβ (1-40) (red; b). Cells are labeled as in Fig. 1D. Scale bars = 2 μm.

B. $K_2Q_{44}K_2$ aggregates induce selective redistribution of CFP-$HttQ_{25}$. HEK293 cells transfected with CFP-$HttQ_{25}$, were incubated with aggregated $K_2Q_{44}K_2$ (c and d), Sup35-NM (e and f), or Aβ(1-40) (g and h). Scale bar = 2 μm.

C. Internalized $K_2Q_{44}K_2$ aggregates induce selective aggregation of cytoplasmic polyQ reporters. Filter retardation assay of HEK293 cells stably expressing the indicated reporters

following incubation with the indicated aggregates (1 μM) for ~ 24 hr or $K_2Q_{44}K_2$ (0.2 μM) as post-lysis control. Data representative of three independent experiments.
D. Infection with Sup35-NM induces selective aggregation of cytoplasmic GFPSup35-NM. *Upper panel*: immunoblot of Sup35-NM sedimentation analysis from HEK293 cells expressing GFP-Sup35-NM exposed to protein aggregates as noted (1μM) prior to lysis and sedimentation into pellet (P) and supernatant (S) fractions. Asterisk, probable proteolysis product. *Bottom panel:* quantification (mean ± SEM) of data from 4 immunoblot experiments. Asterisk, $p \leq 0.0022$.

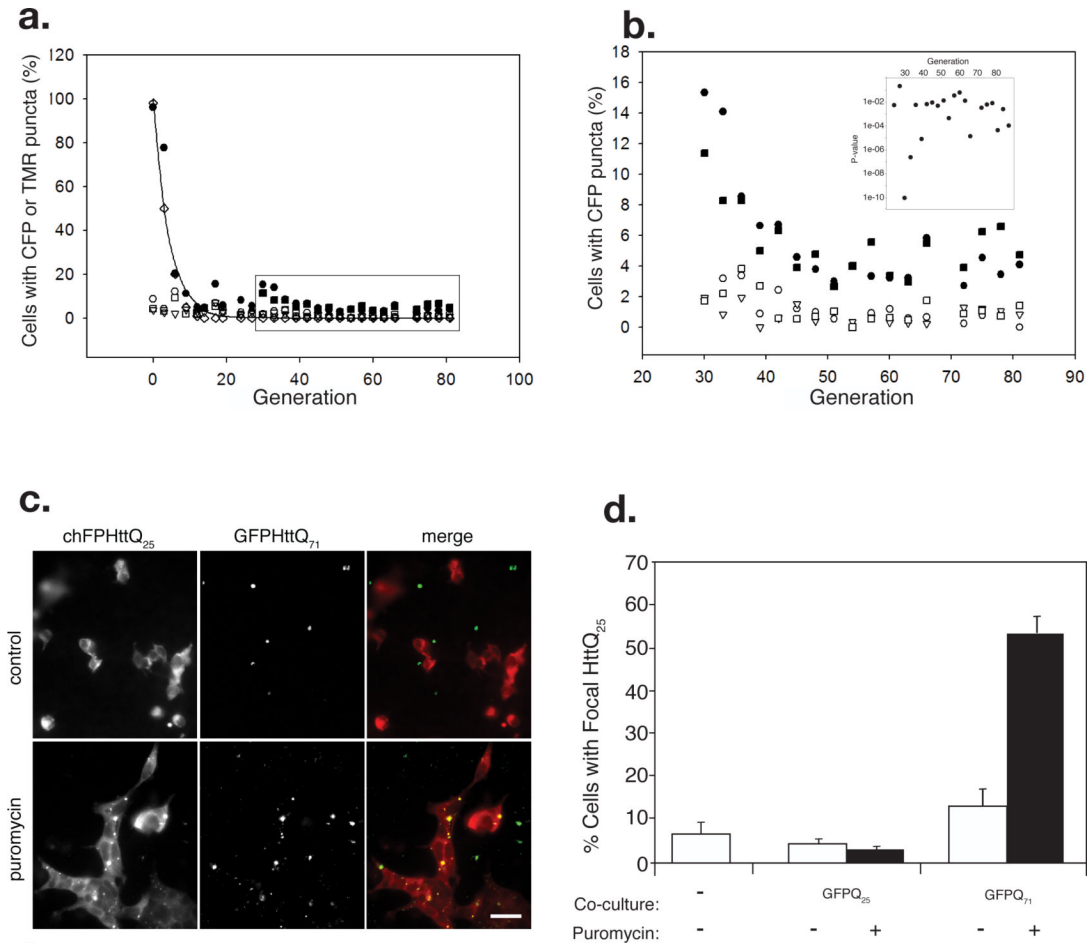


**Figure 4. Propagation of homotypic polyQ aggregation in cell culture**

A. HEK293 cells stably expressing CFP-Htt$Q_{25}$ were exposed to TMR-$K_2Q_{44}K_2$ aggregates (1 μM, solid circles; 0.1 μM, solid squares) or controls: mock infection (open circles), dextran (open triangles), or Aβ aggregates (open squares). Following the indicated number of generations in culture, cells were scored for CFP fluorescence distribution and for the presence of TMR (open diamonds) fluorescence. Each point represents counts of ≥400 cells. The solid line represents the theoretical decay of TMR fluorescence.

B. Blow-up of boxed region from Fig. 4a. Symbols as in Fig. 4a. Data representative of three independent experiments. *Inset*, P-values determined from binomial test of proportions for generations 24-87.

C. Intercellular transfer of polyQ aggregates in mammalian cell co-culture. Puro$^r$ HEK293 cells stably expressing chFP-Htt$Q_{25}$ were cultured together with puromycin-sensitive cells stably expressing GFP-Htt$Q_{71}$. Cells were imaged after 72 hr of co-culture in DMEM (top row) or DMEM containing 4μg/ml puromycin (bottom row). Scale bars = 2 μm.

D. Quantification of chFP-Htt$Q_{25}$ puncta formation in puro$^r$ reporter cells cultured alone or co-cultured with cells stably expressing GFP-Htt$Q_{25}$ or GFP-Htt$Q_{71}$ in the presence or absence of puromycin (4μg/ml). Number of cells counted, $n$ = 699-1276.